

IMECE2015-51706

The Effect Of Raised Benches Containing Crops on the Indoor Environment in Greenhouses

Sunita Kruger

University of Johannesburg
Faculty of Engineering and the Built Environment
Department of Mechanical Engineering Science
University of Johannesburg, PO Box 524,
Auckland Park, 2006
South Africa
skruger@uj.ac.za
Tel: +27 11 559 2066

Leon Pretorius

University of Pretoria
Faculty of Engineering , the Built Environment
and Information Technology , Graduate School of
Technology Management
University of Pretoria, Pretoria, 0002
South Africa
Leon.Pretorius@up.ac.za
Tel: +27 12 420 4148

ABSTRACT

The purpose of this paper is to investigate the influence of peninsular arranged perforated benches containing plants on the indoor environment of a naturally ventilated greenhouse. The results are compared to a greenhouse containing peninsular arranged solid benches with no plants. The investigation will be conducted numerically using three-dimensional Computational Fluid Dynamics (CFD) models. The overall temperature and velocity distribution were investigated at different sections of the greenhouse. The temperature and velocity distributions at plant level were of particular interest. Results indicated that the greenhouse containing the perforated benches were in general cooler, but also exhibited higher velocities throughout. The velocities observed were higher than those recommended by ASHRAE [1]. It was concluded that care should be taken when placing plants on the perforated benches especially in the regions adjacent to the walls, as this can lead to non-uniform crop production.

INTRODUCTION

Greenhouses are crop protecting structures that can be used effectively to protect crops against several unwanted

factors, such as high winds, insects and airborne diseases. Extreme environmental factors such as too high/low temperatures and low humidity are also of concern. The quality of crops in greenhouses is largely influenced by spatial variations in air velocity, temperature and humidity, which are directly influenced by fluctuations in wind flow [2]. In addition to humidity and temperature distribution at plant level, the velocity field and corresponding aerodynamic resistances are also of major importance [3]. The convective heat exchange between the crop and interior air is dictated by air movement, which in turn influences the microclimate around the crops [4]. According to ASHRAE [1] the commonly accepted air speed for plant growth is 0.5 to 0.7m/s. In commercial greenhouses a large variation in indoor climate is often found. This leads to temperature differences which cause non-uniform crop production and quality, as well as problems with pests and diseases [5]. It directly influences the intensity of heat transfer between the air and plant canopy, as well as the intensity of water exchange between the air and the plant canopy. When plants are present inside a naturally ventilated greenhouse, the main effect is to alter the mean velocity [6]. The surrounding aerial, plant and soil environments are directly affected, as the microclimate processes of exchanges of heat, water vapor and carbon dioxide are influenced. The plants can either warm or

cool the ambient air, depending on the radiative energy required for transpiration. [7].

Raised benches are often used in greenhouses to achieve efficient utilization and the maximum amount of growing area. To accomplish this, various raised bench arrangements are commonly used in multi-span greenhouses, such as longitudinal and peninsular arrangements (FIGURE 1).

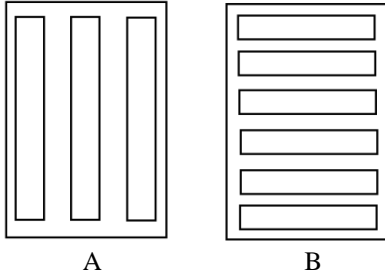


FIGURE 1: A) LONGITUDINAL ARRANGED BENCHES B) PENINSULAR ARRANGED BENCHES

Greenhouse benches have several advantages when compared to cultivating crops directly in the soil: 1) plants are at a convenient level for greenhouse workers 2) plant display is more effective 3) improved air circulation is provided and 4) increased disease and growth control are permitted [8]. The peninsular design allows for segregation of various species, whereas routine tasks such as watering is easier on longitudinally placed benches [9]. It is recommended for efficiency that the bench-to-aisle ratio not exceed 1/3 to 1/4 of the total greenhouse area [8]. The presence of a crop and benches usually has a negative effect on ventilation, as they exert a drag force and induce a momentum loss in the airflow [6]. When a crop is included, it is generally modeled as a porous medium as far as momentum transfer is concerned using the Darcy-Forchheimer equation [10]:

$$S_{\phi} = -\left(\frac{\mu_a}{K}V + \frac{\rho_a C_F}{K^{0.5}}V^2\right) \quad (3)$$

The Darcy-Forchheimer law is valid when $Re > 1$, and for sufficiently high Reynolds numbers, the sink of momentum due to the drag effect of a crop can be expressed by the following equation [11]:

$$S_{\phi} = -\rho_a LADC_D V^2 \quad (4)$$

This equation corresponds to the source term of the Navier-Stokes equation (expressed by unit of volume of the canopy cover). It is generally assumed that a major portion of the total crop canopy drag can be attributed to pressure forces, and

therefore the viscous resistance of the crop (the first term) may be neglected [12]. Combining equations (3) and (4) yields

$$\frac{C_F}{\sqrt{K}} = LADC_D \quad (5)$$

Thus:

$$S_{\phi} = -\rho_a LADC_D V^2 = -\rho_a \frac{C_F}{\sqrt{K}} V^2 \quad (6)$$

Where the leaf area density is defined as:

$$LAD = \frac{LAI}{H} \quad (7)$$

Bench space efficiency (percentage) is defined as follows in equation (1) [5]:

$$\frac{\text{number of benches} \times \text{length of each bench} \times \text{width of bench}}{\text{greenhouse dimensions (width} \times \text{length)}} \times 100 \quad (8)$$

If the bench space efficiency is calculated for both the peninsular and longitudinal layout, it is usually found that the peninsular design allows for more growing area [9].

Computational Fluid Dynamics has become a powerful tool for investigating the distributed climate inside greenhouses. Several authors dedicated time to investigate crop influence in naturally ventilated greenhouses. Roy and Boulard [13] studied the influence of wind direction on a tunnel greenhouse using CFD. Different turbulence models were also studied. A crop model was included with momentum, heat and humidity transfers between the crop and inside airflow. The influence of wind conditions was illustrated. The microclimate characteristics and transpiration of an Impatiens pot plant crop in a greenhouse were studied both numerically and experimentally by Kichah et al [14]. The model they developed could be useful for irrigation management. The effect of cover properties, ventilation rate and crop leaf area on tropical greenhouse climate was investigated by Impron et al [15]. Their measurements and calculations showed that the temperature of the greenhouse air was more affected by variations in ventilation and leaf area index than the cover properties. It was also concluded that the leaf area index had the most significant effect on greenhouse air temperature, which implies that a large proportion of the cooling is achieved by the crop.

The objective of this paper is to numerically investigate the influence of peninsular arranged perforated benches containing potted plants on the indoor climate of naturally ventilated greenhouse. This will be compared to a greenhouse containing only solid benches, also arranged in a peninsular manner.

COMPUTATIONAL FLUID DYNAMICS

The first numerical simulations using CFD on greenhouse ventilation were conducted by Okushima et al [16]. Although little correlation was found between the wind tunnel and CFD results, the results nonetheless provided significant information regarding the flow inside greenhouses. Development in computer technology increased the popularity of numerical methods as a tool to investigate the microclimate inside greenhouses. In Computational Fluid Dynamics a numerical solution of partial differential equations governing the transport of mass, momentum and energy in moving fluids is obtained [17]. The first step in this approach to solve the transport equations is finite volume discretization. This method subdivides the solution domain into a finite number of small control volumes, which corresponds to the cells of a computational grid. Discrete versions of the integral form of the continuum transport equations are applied to each volume. The objective of this method is to obtain a set of algebraic equations. An algebraic multi-grid solver such as the one described in [18] can then be used to solve the resulting equations. To illustrate this, the transport of a simple scalar will be considered. The continuous Integral form of the governing equation is typically given by Eq. (1) [18]:

$$\frac{d}{dt} \int_V \rho \phi dV + \oint_A \rho \phi (\bar{v} - \bar{v}_g) \cdot d\bar{a} = \oint_A \Gamma \nabla \phi \cdot d\bar{a} + \int_V S_\phi dV \quad (9)$$

The first term is the transient term, which is generally only included in transient calculations. The second term is the convective flux, third term the diffusive flux, and lastly the volumetric source term. The mathematical formulation of each term is also defined in the StarCCM+ documentation, as well as in for instance Versteeg et al [19]. If Eq. 9 is discretized, the following equation results:

$$\frac{d}{dt} (\rho \phi V)_0 + \sum_f [\rho \phi (\bar{v} \cdot \bar{a} - G)]_f = \sum_f (\Gamma \nabla \phi \cdot \bar{a})_f + (S_\phi V)_0 \quad (10)$$

The discretization procedure is discussed in more detail in Patankar [20].

NUMERICAL MODEL

The commercial CFD code StarCCM+ [18] was used to perform the numerical analysis presented in this paper. The greenhouse studied in this paper is based on a greenhouse found in the literature [21] and has already been validated previously [9]. This greenhouse contained four spans (width, 4 by 9.60m; length, 68m; eaves' height, 3.90m; ridge height, 5.9m) and was covered by 4mm thick horticulture glass (FIGURE 2). The greenhouse roof was equipped with continuous roof vents on both sides of each span. The ventilator openings were assumed to be 1.22m wide [1]. In order to simplify the analysis in this paper, only the first two spans were

investigated. The ventilator openings were assumed to be 1.22m wide [22]. The greenhouse in the CFD model was only 20m in length and contained 2 spans of 9.6m each. The origin was chosen as the bottom left corner, at the back of the greenhouse as shown in Figure 2. The initial greenhouse contained 24 solid benches without plants and the second greenhouse contained 24 peninsular arranged raised benches containing potted Impatiens, 0.45m high, shown in Figure 4. This equated to a bench space efficiency of 42%.

Porous Media Formulation

In StarCCM+, the porous source term appears in the momentum equations of the coupled solver and is defined by eq 11 [18]:

$$\mathbf{f}_p = -\mathbf{P} \cdot \mathbf{v} \quad (11)$$

Where \mathbf{P} is the porous resistance tensor. The porous resistance tensor is defined by:

$$\mathbf{P} = \mathbf{P}_v + \mathbf{P}_i |\mathbf{v}| \quad (12)$$

\mathbf{P}_v and \mathbf{P}_i are the viscous (linear) and inertial (quadratic) resistance tensors respectively [18]. The flow velocity through the porous region (plants) was related to the pressure gradient by applying the Dupuit and Forchheimer equation [18]:

$$-\nabla p = \frac{\mu}{k_p} \mathbf{v} + \beta \rho \mathbf{v}^2 \quad (11)$$

If this equation is compared to equation 3, the similarity is notable. The constant β must be evaluated depending on the flow and medium of interest, commonly deduced by experiments. The leaf area index of the Impatiens was found to be 3.95m² of leaves per m² of ground by Kicah et al [14]. As already mentioned, the linear term in Equation 11 can be ignored, therefore the coefficient for the quadratic term had to be determined. The density of the air was taken as 1.204kg/m³, and the drag coefficient $C_D = 0.32$ as discussed in [14].

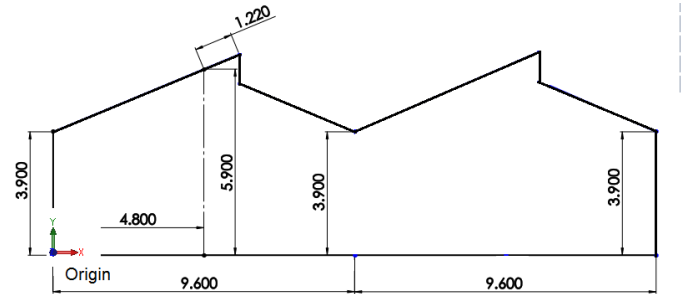


FIGURE 2: GREENHOUSE DIMENSIONS [21]

A large computational control volume shown in FIGURE 3 (250m x 100m x 100m) was created around the greenhouse in the CFD analysis to ensure minimal interference from the

boundaries on the flow inside the greenhouse and to allow for development and definition of the boundary layer. The negative y-direction was chosen as the direction of the gravitational constant for all the greenhouse models in this paper. The wind was modelled to act from left to right in an eastern direction at 1m/s for each case. This was done for comparison purposes with the original validated greenhouse [21]. The wind velocity was chosen for comparison purposes with the original validated greenhouse [21].

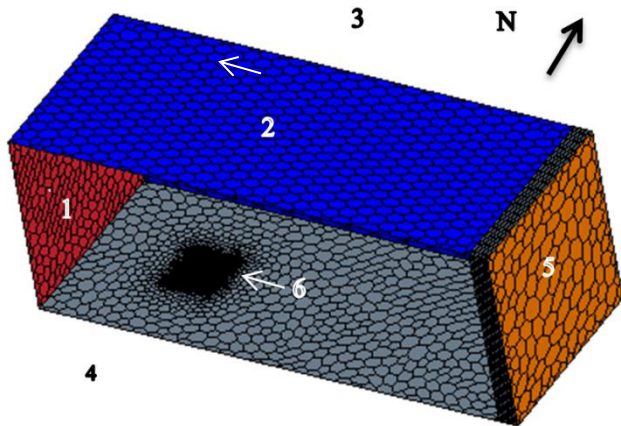


FIGURE 3: CONTROL VOLUME AROUND GREENHOUSE

The outlet of the domain was specified as a porous region, using the mesh extruder in StarCCM+ in order to force the flow out of the domain. This is an artificial boundary created to ensure a positive pressure over the outlet boundary, to avoid recirculating flow developing. As the outlet boundary is far from the region of interest, the effect on the solution was considered negligible. A summary of the boundary conditions can be seen in Table 1.

TABLE 1: SUMMARY OF BOUNDARY CONDITIONS

Nr	Boundary Name	Boundary Type
1	Inlet	Velocity Inlet
2,3,4	Top, front, back	Symmetry Plane
5	Outlet	Pressure Outlet
6	Glass Walls	Baffle Interfaces

The porous region was 10m, with 10 orthogonal extruded cells, which was extruded from the volume mesh at the outlet boundary. The mesh around and behind the greenhouse was refined using a volume source to 3% of the base size, while the mesh around the benches containing the plants was further refined with a volume source to 1.5% of the base size. A meshed 3D model of a leeward-facing (ventilators) greenhouse containing longitudinal benches is shown in FIGURE 4. The glass walls of the greenhouse were modelled as baffle interfaces with an effective thermal resistance. A baffle interface physically represents one or more thin sheets of

impermeable, conducting materials in a fluid, with an infinitesimal thickness [18]. A cut-away view is shown in Fig. 5 of the mesh inside greenhouse and around the raised benches containing the plants.

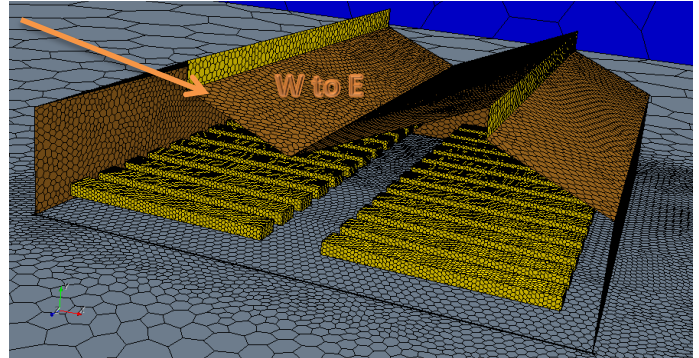


FIGURE 4: MESHED GREENHOUSE WITH ORIENTATION

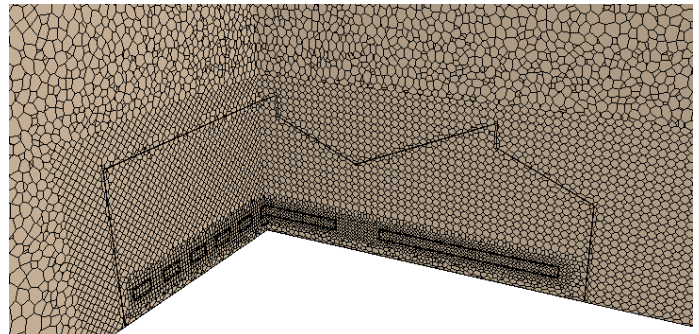


FIGURE 5: CUT-AWAY VIEW OF MESH INSIDE GREENHOUSE

The domain was meshed using a polyhedral meshing model (FIGURE 5), together with a boundary layer meshing model. The prism layer model was activated to ensure adequate modelling of the flow in the boundary layer. After monitoring the wall Y+ values on the walls of the greenhouse, the prism layer mesh was created, consisting of 10 orthogonal prismatic cells, with a thickness of 0.1m. The prism layer was present on all the wall type boundaries in the solution domain as well as the baffle interfaces. A tetrahedral mesh was created initially, after which a special dualization scheme was implemented to generate the polyhedral mesh, which consists of arbitrary shaped polyhedral cells. A mesh sensitivity analysis was conducted to ensure mesh independence. Taking running time and convergence into consideration, it was decided to use a final base size 10m for all the simulations.

The turbulent nature for both inner and outer flows of greenhouses was confirmed by Boulard et al [23]. In StarCCM+ turbulence is also simulated by solving the Reynolds-averaged governing equations for momentum, energy and scalar transport. For this investigation the realizable k-epsilon model was implemented developed by Shih et al [24] and combined with the two-layer approach. This combination

has the added flexibility of an all Y+ wall treatment [18] and allows the k-epsilon model to be applied in the viscous sublayer. Numerical probes were inserted at various points in the flow in the CFD model, and the solution monitored for convergence. The input boundary and other parameters from Ould Khaoua [21] used in the simulations are shown in Table 2.

TABLE 2: INPUT VALUES FOR CFD SIMULATIONS

<i>Parameter</i>	<i>Unit</i>	<i>Value</i>
Inlet Air		
Temperature	°C	22.2
Outside Ground	°C	27.9
Inside Ground	°C	27.3
Effective Thermal Resistance	W/m ²	0.00286

Two cases were investigated numerically – the first case (Case 1) contained a leeward facing greenhouse with peninsular arranged solid benches, and the second case (Case 2) was concerned with a leeward facing greenhouse with peninsular arranged perforated benches containing plants. The velocity and temperature were evaluated at a height of 1.4m, which is just above the plant level for the greenhouse containing the plants.

RESULTS

Results are presented in the form of velocity vector, contour plots and graphs. The numerical temperature contour plots at a height of 1.4m are compared in FIGURE 6. In general it can be seen that the temperature at plant level is higher for the solid bench case compared to the perforated benches containing the plants. Slightly higher temperatures are noticed towards the left of the greenhouse, the core of the greenhouse, and adjacent to the right wall for the second case. When the velocity contour plots are compared (FIGURE 7), the velocity in the case where there is only solid benches is generally much lower compared to the case with the perforated benches. In the second case, relatively high velocities (in the region of 2m/s) are noticed adjacent to the walls, and against back and front walls there are areas where the velocity reaches up to 3.6m/s. The warmer indoor environment in Case 1 can be attributed to the low velocities observed.

FIGURE 8 compares the velocity contour plots and vectors for three different planes in the greenhouse, measured from the back of the greenhouse (5m,10m, and 15m respectively). All three planes exhibit a lower velocity compared to the same plane in the case with the perforated benches and plants. For Case 1, the highest velocity (although lower compared to case 2) at the 5m plane occurs adjacent to the roof, the right wall, and the floor of the second span.

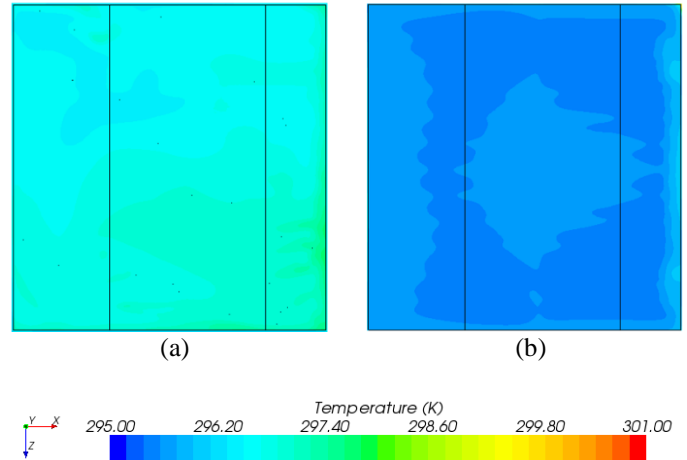


FIGURE 6: TEMPERATURE CONTOUR PLOTS FOR a) CASE 1 b) CASE 2

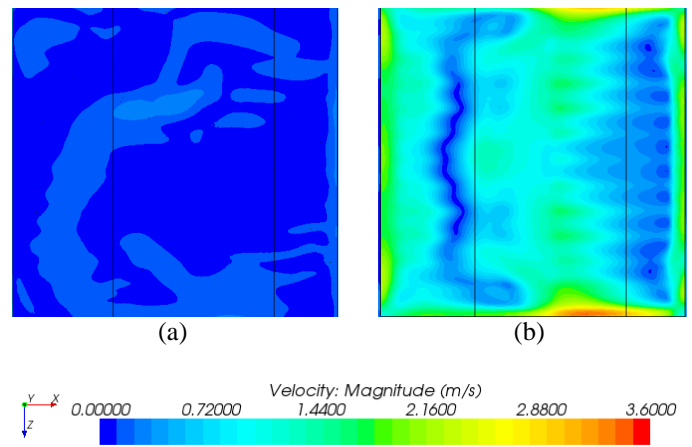


FIGURE 7: VELOCITY CONTOUR PLOTS FOR A) CASE 1 B) CASE 2

Air is sucked in through the roof ventilator in this plane, falls down to the floor and splits into two streams. Some of the air moves underneath the second bench towards and up the right wall, where it joins the fresh air flow moving into the ventilator. For the plane at 10m from the back of the greenhouse, the air also moves into the greenhouse at the second ventilator, but as the flow patterns are three dimensional, one cannot fully distinguish the flow patterns in a particular plane. It is also noticed that highest velocities are on the floor in the first span, and adjacent to the right wall and the roof. Flow moves into the second ventilator, but out of the first ventilator in the 15m plane.

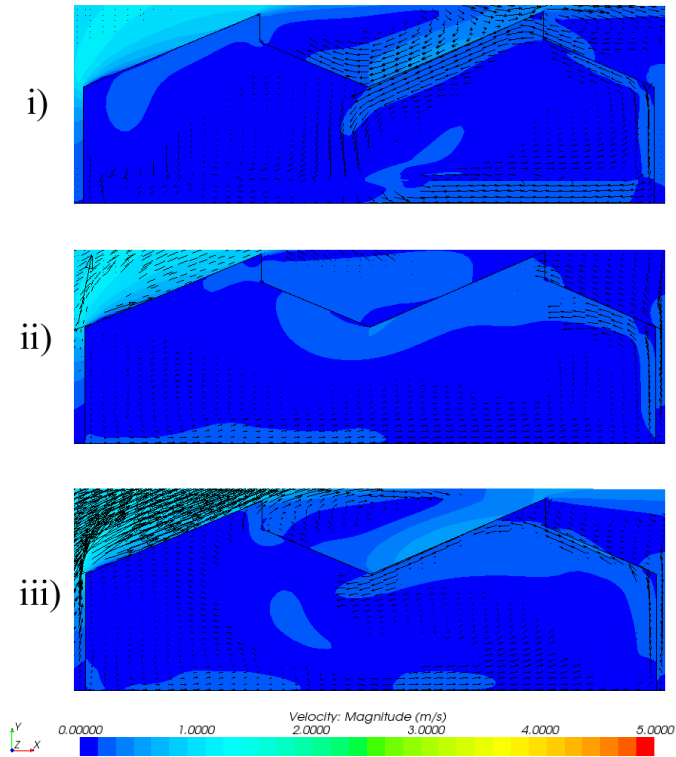


FIGURE 8: VELOCITY CONTOURS AND VECTORS AT I) 5M II)10M III) 15M FROM THE BACK OF THE GREENHOUSE (CASE 1)

The velocity contour and vector plots for the second case are shown in FIGURE 9. Velocities as high as 4m/s are observed, especially near the roof where the air enters through the ventilators. At 5m, the air is sucked in through the second ventilator, and moves adjacent to the roof, where it falls to the floor in the center of the greenhouse, and a clear counter clockwise cell is formed in the second span of the greenhouse. High velocities (approximately 1.4m/s) are noticed on top of the shelf in both the first and the second span. The second shelf also has a stagnant region forming towards the right of the shelf. The air velocity also enters the first ventilator at a relatively high speed compared to the rest of the greenhouse, and moves down against the left wall. The air is seen to move underneath the shelves from left to right at a high speed. If the plane at 10m is investigated, the velocity vectors are less visible compared to the 5m plane, indicating that the flow is three-dimensional. Air is sucked in through both roof ventilators in this plane. Lastly, at the 15m plane, the direction of the flow at the ventilators is not clear, but a large counter-clockwise convective cell forms in the first span, forcing flow along the floor towards the right of the greenhouse, where it moves up the right wall. Two stagnant regions are noticed, one in each span, and adjacent to the second half of the first span roof.

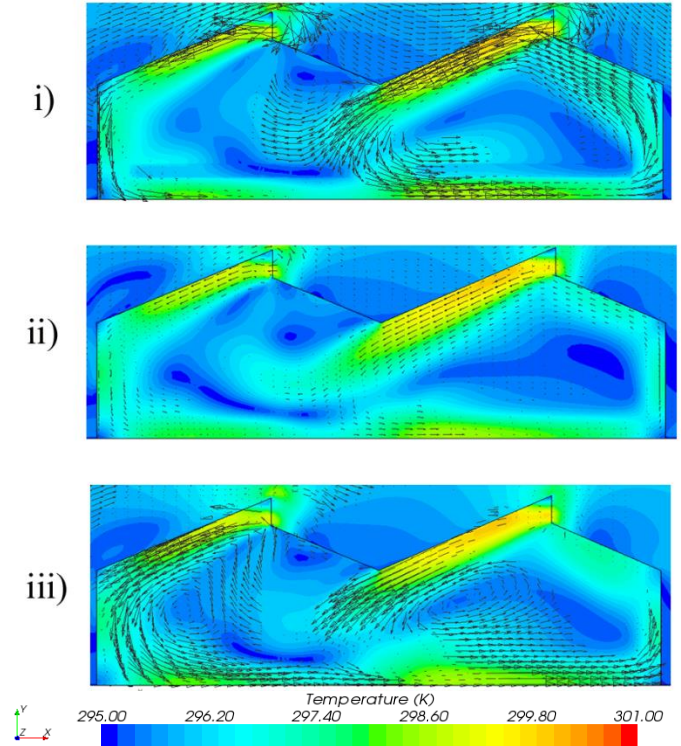


FIGURE 9: VELOCITY CONTOURS AND VECTORS AT I) 5M II)10M III) 15M FROM THE BACK OF THE GREENHOUSE (CASE 2)

The temperature distribution at plant level (1.4m) in the three planes (5m,10m and 15m) are compared in FIGURE 10. It can be observed that the temperature increases slightly towards the front of the greenhouse. Each plane exhibits a high temperature gradient adjacent to the right wall.

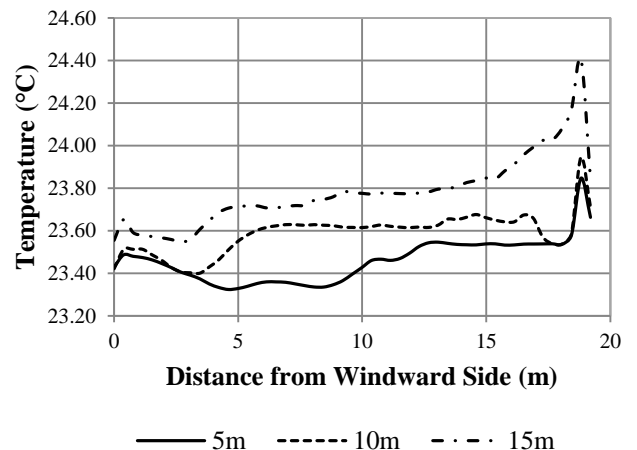


FIGURE 10: TEMPERATURE COMPARISON FOR CASE 1 AT PLANT LEVEL

FIGURE 11 displays the temperature comparison for Case 2 at plant level for the three planes. The temperature is more

homogeneously distributed compared to case 1, and it can be seen that the 5m and 15m displays similar behavior. High temperature gradients are visible adjacent to both walls.

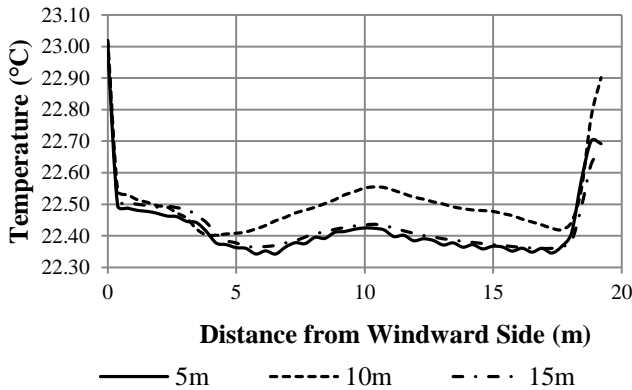


FIGURE 11: TEMPERATURE COMPARISON FOR CASE 2 AT PLANT LEVEL

The temperature distribution at plant level (1.4m) for the case with the solid benches (Case 1) is compared in FIGURE 12 to the case for perforated benches with plants. In general, the temperature is about 4% lower in case of the perforated benches with plants. Both distributions are homogeneous with a slight temperature rise at the right wall, while the a temperature drop of approximately 0.6°C is noticed adjacent to the left wall for Case 2.



FIGURE 12: TEMPERATURE DISTRIBUTION COMPARISON AT 5M

The temperatures in the 10m plant at plant level are compared in FIGURE 13. Both distributions are relatively homogenous, but on average the temperature in Case 1 with the solid benches are 4.6% higher compared to Case 2. Case 2 also displays a temperature gradient at both walls, whereas Case 1 has a slight temperature gradient at the right wall of approximately 0.4°C.

FIGURE 14 shows the temperature comparison at plant level for the 15m plant (front of the greenhouse). The temperature distribution in the greenhouse containing the solid benches are on average 5.6% higher compared to the temperatures in the greenhouse containing the benches with the plants. A maximum temperature of 24.4°C is reached in the greenhouse with the solid benches towards the right wall.

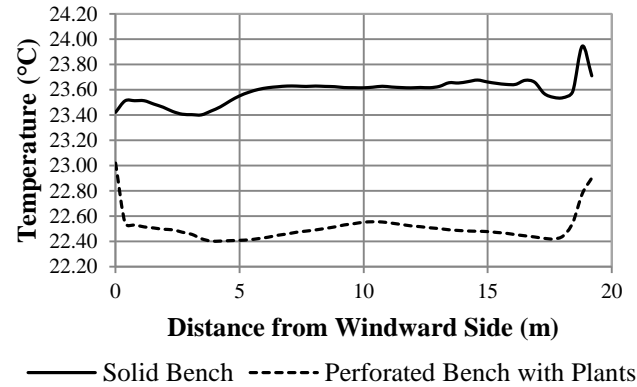


FIGURE 13: TEMPERATURE DISTRIBUTION COMPARISON AT 10M

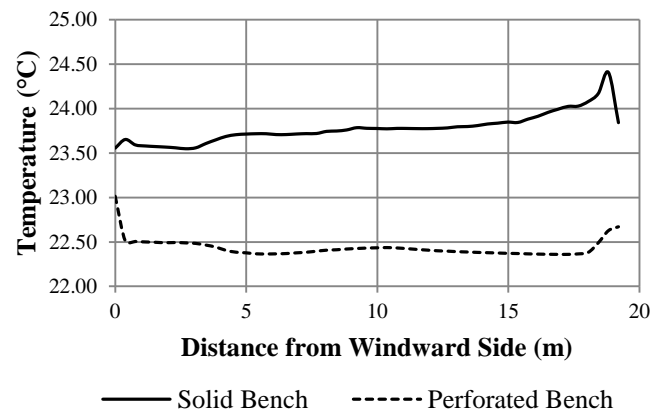


FIGURE 14: TEMPERATURE COMPARISON AT 15M

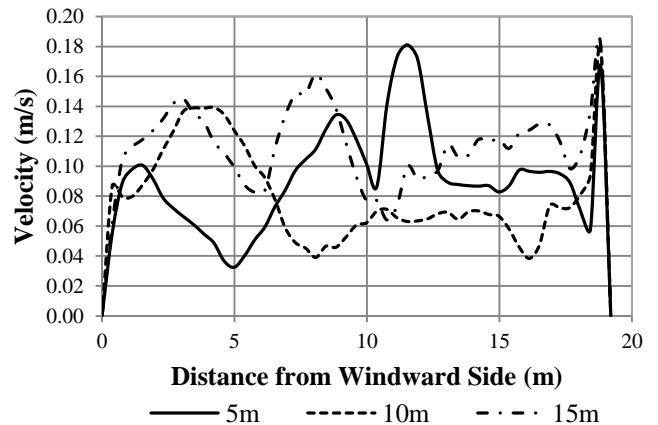


FIGURE 15: VELOCITY COMPARISON FOR CASE 1 AT PLANT LEVEL

A plot of the velocity comparison at plant level is shown in FIGURE 15. The velocity distribution is heterogeneous throughout the greenhouse, and varies from close to 0m/s to a maximum of 0.18m/s in the 15m span. FIGURE 16 compares the velocity distribution at plant level for case 2. A similar trend is noticed for all three planes – a maximum is reached in each plane close to the walls, while a second maximum is reached toward the center of the greenhouse. The velocity distribution for the 10m plane is slightly skew, as the maximum is reached at approximately 6m from the windward side.

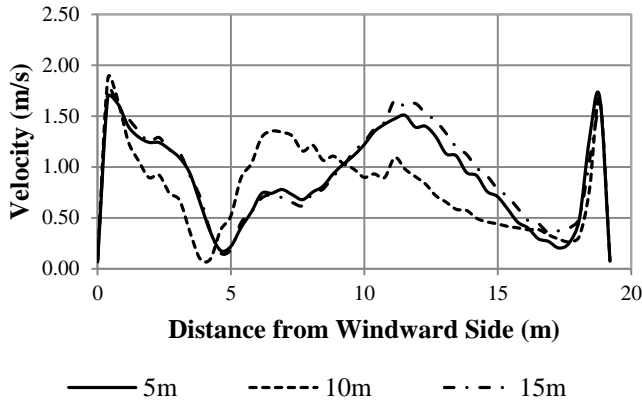


FIGURE 16: VELOCITY COMPARISON FOR CASE 2 AT PLANT LEVEL

If the individual planes are compared for the two cases, it is observed from FIGURE 17 that the velocity is on average higher (90%) for the case containing the benches with the plants compared to the case with the solid benches. The velocity distribution in the second case reaches a maximum close to the walls of approximately 1.7m/s, with a second maximum of 1.5m/s reached at the center of the greenhouse. These velocities are higher than recommended for plant growth.

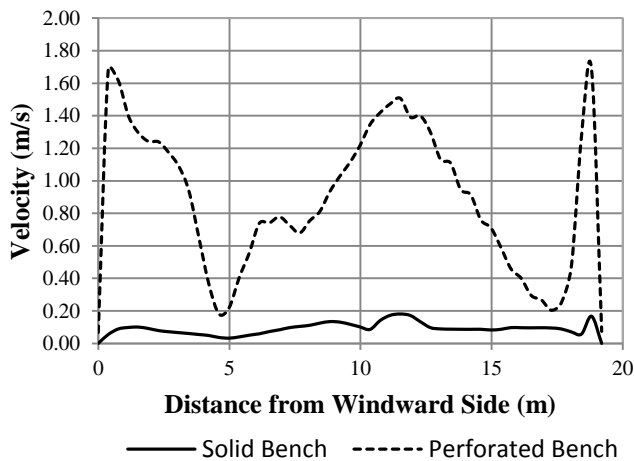


FIGURE 17: VELOCITY DISTRIBUTION COMPARISON AT 5M

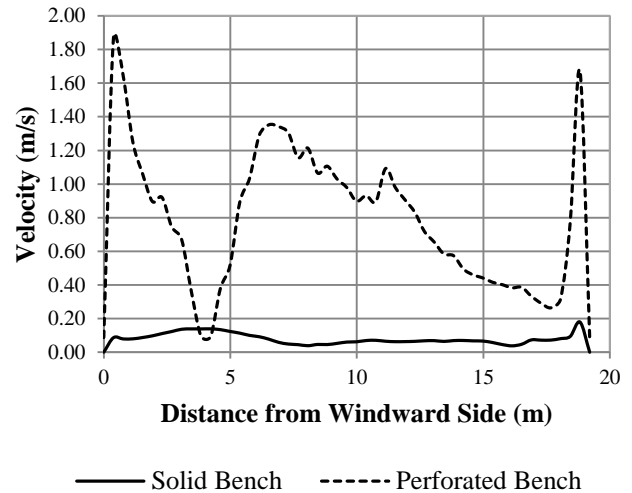


FIGURE 18: VELOCITY DISTRIBUTION COMPARISON AT 10M

FIGURE 18 plots the velocity distribution at plant level at the 10m plane. Once again, the velocity distribution on average for Case 2 is higher (90%) compared to Case 1. One can see that there is almost no movement of air at plant level for the case with the solid benches. Case 2 also reaches a maximum velocity close to the walls of approximately 1.8m/s close to the left wall, and 1.7m/s close to the right wall respectively. The higher temperatures in Case 1 can be attributed to the low velocity at plant level. A similar trend is exhibited by the distribution at the 15m plane (FIGURE 19). In all three planes, the velocities near the walls are too high according to ASHRAE [1].



FIGURE 19: VELOCITY DISTRIBUTION COMPARISON AT 15M

CONCLUSION

In this paper, three-dimensional CFD models were used to numerically investigate the indoor climate of a naturally ventilated greenhouse containing peninsular arranged

perforated benches with plants. This CFD model was compared to a CFD model of a similar greenhouse containing only solid benches with no plants.

In general, it was found that the presence of benches containing a crop significantly influenced the velocity and temperature distribution not only at plant level, but the entire indoor climate of the greenhouse. The greenhouse containing the solid benches was in general much warmer compared to the greenhouse with the perforated benches and the plants. Overall a lower velocity was also noticed for Case 1. The higher temperatures could be attributed to the stagnant areas and low velocity distribution.

The velocities observed in the greenhouse containing the perforated benches and crop was almost 90% higher compared to the solid bench greenhouse. These velocities are higher than the commonly accepted air speed for plant growth. The higher velocities in Case 2 could be attributed to the stagnant recirculating areas forming on top of the solid benches. Therefore, care should be taken especially when placing plants adjacent to the walls, as all the planes exhibit high air velocities in these regions. This could lead to non-uniform crop production.

Current results were generated as part of an exploratory research study on three-dimensional effects in greenhouse microclimates. Future research may include the effect of wind direction in three-dimensions. The glass walls can also be modelled with a finite thickness instead of baffles, to further investigate the heat transfer through the greenhouse cover.

NOMENCLATURE

\bar{a}		Coefficient arising from Finite Volume Discretization
C_D	-	Drag Coefficient
C_F	-	Non-linear Momentum Loss Coefficient
G		Grid flux computed from mesh motion
LAD	$[m^2/m^3]$	Leaf Area Density
LAI	$[m^2/m^2]$	Leaf Area Index (m^2 of leaves by m^2 of ground covered by the crop)
k_p	$[m^2]$	Permeability
S_ϕ		Source Term
v	$[m/s]$	Superficial velocity through medium
V	$[m/s]$	Modulus of the air speed
\bar{v}	$[m/s]$	Velocity
\bar{v}_g	$[m/s]$	Grid velocity
ρ	$[kg/m^3]$	Density
Φ	*	Scalar Quantity
Γ	*	Diffusion Coefficient
μ	$[kg/m.s]$	Fluid Molecular Viscosity
Subscripts		
a	-	Air
* For units refer to the StarCCM+ Documentation [18]		

REFERENCES

- [1] ASHRAE, "Fundamentals," in *2005 ASHRAE Fundamentals Handbook*, Atlanta, ASHRAE, 2005.
- [2] T. Boulard, S. Wang and R. Haxaire, "Mean and Turbulent Air Flows and Microclimatic patterns in an empty greenhouse tunnel," *Agricultural and Forest Meteorology*, vol. 100, pp. 169-181, 2000.
- [3] P. E. Bournet and T. Boulard, "Effect of ventilator configuration on the distributed climate of greenhouses: A review of experimental and CFD studies," *Computers and Electronics in Agriculture*, vol. 74, pp. pp 195 - 217, 2010.
- [4] S. Wang, T. Boulard and R. Haxaire, "Air speed profiles in a naturally ventilated greenhouse with a tomato crop," *Agricultural and Forest Meteorology*, vol. 96, pp. pp 181-188, 1999.
- [5] K. Popovski, "Greenhouse Climate Factors," *GHC Bulletin*, January 1997.
- [6] F. D. Molina-Aiz, D. L. Valera, A. J. Alvarez and A. Madueno, "A Wind Tunnel Study of Airflow through Horticultural Crops: Determination of the Drag Coefficient," *Biosystems Engineering*, vol. 93, no. 4, pp. 447 - 457, 2006.
- [7] "Measurement and CFD simulation of microclimate characteristics and transpiration of an Impatiens pot plant crop in a greenhouse," *Biosystems Engineering*, vol. 112, pp. 22-34, 2012.
- [8] J. N. Walker and G. A. Duncan, "Greenhouse Benches," [Online]. Available: <http://www.bae.uky.edu/publications/aens.asp>. [Accessed 18 April 2013].
- [9] M. A. Schnelle and J. M. Dole, "Greenhouse Floors and Benches - OSU Fact Sheets," [Online]. Available: <http://osufacts.okstate.edu>. [Accessed 15 January 2013].
- [10] T. Boulard and W. S., "Experimental and numerical studies on the heterogeneity of crop transpiration in a plastic tunnel," *Computers and Electronics in Agriculture*.
- [11] A. S. Thom, "Momentum absorption by vegetation," *Quarterly Journal of the Royal Meteorological Society*, vol. 97, pp. 414-428, 1971.
- [12] T. Bartzanas, T. Boulard and C. Kittas, "Effect of Vent Arrangement on Windward Ventilation of a Tunnel Greenhouse," *Biosystems Engineering*, vol. 2, pp. pp 479-490, 2004.
- [13] J. C. Roy and T. Boulard, "CFD Prediction of the Natural Ventilation in a Tunnel-Type Greenhouse: Influence of Wind Direction and Sensibility to Turbulence Models," *Acta Hort 691*, 2005.
- [14] A. Kichah, P. E. Bournet, C. Migeon and T. Boulard, "Measurement and CFD simulation of microclimate characteristics and transpiration of an Impatiens pot plant crop in a greenhouse," *Biosystems Engineering*, vol. 112,

- pp. pp 22 - 34, 2012.
- [15] I. Impron, S. Hemming and G. P. Bot, "Effects of cover properties, ventilation rate, and crop leaf area on tropical greenhouse climate," *Biosystems Engineering*, vol. 99, pp. pp 553 - 564, 2008.
- [16] L. Okushima, S. Sase and M. Nara, "A support system for natural ventilation design of greenhouses based on computational aerodynamics," *Acta Horti*, vol. 284, pp. 129-136, 1989.
- [17] I. H. Shames, *Mechanics of Fluids*, New York: McGraw-Hill, 2003.
- [18] CD-Adapco, "Star CCM+ User Guide," CD-Adapco, 2012.
- [19] H. K. Versteeg and W. Malalasekera, *An introduction to Computational Fluid Dynamics, The Finite Volume Method*, 2nd Ed, England: Pearson Prentice Hall, 2007.
- [20] S. V. Patankar, *Numerical Fluid Flow and Heat Transfer*, New York: Hemisphere, 1980.
- [21] S. Ould Khaoua, P. Bournet, C. Migeon and G. Chasseriaux, "Analysis of Greenhouse Ventilation Efficiency based on Computational Fluid Dynamics," *Biosystems Engineering*, pp. 83-98, 2006.
- [22] J. W. Boodley, *The Commercial Greenhouse*, New York: Delmar Publishers, 1998.
- [23] T. Boulard, S. Wang and R. Haxaire, "Mean and Turbulent air flows and microclimatic patterns in an empty greenhouse tunnel," *Agricultural and Forest Meteorology*, vol. 100, p. 169 – 181, 2000.
- [24] T. Shih, W. W. Liou, A. Shabbitt, Z. Zang and J. Zhu, "A New k-epsilon Eddy Viscosity Model for High Reynolds Number Turbulent Flows," NASA, 1994.
- [25] P. Bournet and T. Boulard, "Effect of ventilator configuration on the distributed climate of greenhouses: A review of experimental and CFD studies," *Computers and Electronics in Agriculture*, vol. 74, pp. 195-217, 2010.